Inertial active Ornstein-Uhlenbeck particle in the presence of a magnetic field

M. Muhsin and M. Sahoo [*]
Department of Physics, University of Kerala, Kariavattom, Thiruvananthapuram 695581, India

(Received 7 January 2022; accepted 29 June 2022; published 20 July 2022)

We consider an inertial active Ornstein-Uhlenbeck particle in an athermal bath. The particle is charged, constrained to move in a two-dimensional harmonic trap, and a magnetic field is applied perpendicular to the plane of motion. The steady-state correlations and the mean-square displacement are studied when the particle is confined as well as when it is set free from the trap. With the help of both numerical simulation and analytical calculations, we observe that inertia plays a crucial role in the dynamics in the presence of a magnetic field. In a highly viscous medium where the inertial effects are negligible, the magnetic field has no influence on the correlated behavior of position as well as velocity. In the time asymptotic limit, the overall displacement of the confined harmonic particle gets enhanced by the presence of a magnetic field and saturates for a stronger magnetic field. On the other hand, when the particle is set free, the overall displacement gets suppressed and approaches zero when the strength of the field is very high. Interestingly, it is seen that in the time asymptotic limit, the confined harmonic particle behaves like a passive particle and becomes independent of the activity, especially in the presence of a very strong magnetic field. Similarly, for a free particle the mean-square displacement in the long time limit becomes independent of activity even for a longer persistence of noise correlation in the dynamics.

DOI: 10.1103/PhysRevE.106.014605

I. INTRODUCTION

Recently, research on active matter has emerged as a vital area of research and attracted much attention in various fields of science [1–4]. Active matter is a special class of nonequilibrium systems which is inherently or intrinsically driven far away from equilibrium. The particles in such a system are capable of self-propelling in the environment. They consume energy from the environment by means of their internal mechanisms and generate a spontaneous flow in the system [4,5]. These particles are termed active or self-propelling particles. Examples of active matter include motile biological microorganisms such as bacteria or unicellular protozoa [6–8], artificially synthesized microswimmers such as Janus particles [9,10], microrobots, hexbugs [11], etc. There exist some standard models such as the active Brownian particle (ABP) model to treat the dynamics of such particles at both the single-particle level and the collective level [12–16]. Recently, a simple and nontrivial model known as the active Ornstein-Uhlenbeck particle (AOUP) model [17–19] was proposed for modeling the overdamped dynamics of such self-propelled particles. In the ABP model, both the translational and the rotational diffusion of the particles are taken into account, while in the AOUP model, the velocity of the particle follows the Ornstein-Uhlenbeck process. The AOUP model has been explored in detail as it makes the exact analytical calculations possible [20–26]. Both these models are successful in explaining many important features of active matter such as accumulation near boundary [27,28], motility-induced phase separation [29] etc. Unfortunately, inertia, which is an important property of physical systems, was not initially considered in these models.

For macroscopic or massive self-propelling particles moving in a gaseous or low-viscous medium, inertial effects become prominent and this poses some new challenges in the theoretical modeling of this kind of system. Typically, millimeter-size particles moving in a low-viscous medium are strongly influenced by inertia. Macroscopic swimmers [30–32] and flying insects [33] are apt examples where inertia plays an important role in their dynamics, at both the single-particle level and the collective level [16]. Hence, inertia needs to be introduced in both AOUP and ABP models. Indeed, in some of the recent works, the introduction of inertia in these models could describe well the dynamics of active particles [34,35]. It has also been reported that fine tuning of inertia results in qualitative modification in the fundamental properties of active systems such as inertial delay between orientation dynamics and translational velocity of active particles [36], development of different dynamical states [37], motility induced temperature difference coexisting phases [38], etc.

The stochastic dynamics of a charged particle in the presence of a magnetic field is an interesting problem with potential applications in plasma physics, astrophysics, electromagnetic theory, etc. [39–45]. According to the Bohr–van Leeuwen theorem [46–49], there is no orbital magnetism for a classical system of charged particles in equilibrium. However, when an inertial system exhibits activity in the dynamics, it does not follow the well known fluctuation-dissipation theorem [50] and comes out of equilibrium. As a result, a nonzero orbital magnetism appears in the presence of a magnetic field and the system passes through a magnetic phase transition depending on the complex interplay of the activity time and other timescales involved in the dynamics [51,52].

[*]jolly.iopb@gmail.com

When a time-dependent magnetic field is applied to charged Brownian swimmers, it can either enhance or reduce the effective diffusion of swimmers [53]. On the other hand, the dynamics of a charged active Brownian particle subjected to a space-dependent magnetic field induces inhomogeneity and flux in the system [54]. Similarly, under stochastic resetting, an active system in the presence of a magnetic field yields some exotic steady-state behavior [55]. Motivated by these recent findings, herein we explore the transport properties of a charged and inertial active Ornstein-Uhlenbeck particle in a viscous medium and under a static magnetic field. In particular, we show that inertia is necessary for the magnetic field to influence the dynamics.

The Brownian dynamics of an inertial charged particle in a magnetic field driven by an exponentially correlated noise and by a colored Gaussian thermal noise has already been discussed in Refs. [56–61], respectively. In these models, the dynamics is always mapped to its thermal equilibrium limit, where the generalized fluctuation-dissipation relation is satisfied. In our work we consider the model as the dynamics of an active particle, which is different from the dynamics described in the previously discussed models in the sense that the active fluctuations are athermal and hence cannot always be mapped to an equilibrium limit. However, in the equilibrium limit of our model, where the fluctuation-dissipation relation is satisfied and in the vanishing limit of noise correlation time, some of our findings, especially the steady-state diffusion, show behavior similar to that reported in Refs. [56,57] for a free particle and in Refs. [58,60] for a confined harmonic particle.

We have organized the paper in the following way. In Sec. II we present our model, the methodology adopted, and an introduction to the dynamical parameters of interest. The results and a discussion are presented in Sec. III, followed by a summary in Sec. IV.

II. MODEL AND METHOD

We consider a charged active Ornstein-Uhlenbeck particle of mass m self-propelling in a two-dimensional (2D) plane. The particle is confined by a harmonic potential $U(x, y) = \frac{1}{2}k(x^2 + y^2)$, with k being the harmonic constant. A magnetic field $\mathbf{B} = B\hat{\mathbf{z}}$ is applied perpendicular to the plane of the motion of particle, where $\hat{\mathbf{z}}$ is the unit vector along the Z direction. The dynamics of the particle is given by Langevin's equation of motion [49,52,62]

$$m\ddot{\mathbf{r}}(t) = -\gamma\mathbf{v}(t) + \frac{|q|}{c}[\mathbf{v(t)} \times \mathbf{B}] - k\mathbf{r}(t) + \sqrt{2D}\xi(t), \quad (1)$$

where $\ddot{\mathbf{r}} = \dot{\mathbf{v}}$ is the acceleration of the particle and $m\ddot{\mathbf{r}}$ is the inertial force in the dynamics. The first term on the right-hand side of Eq. (1) is the viscous force on the particle because of the interaction of the particle with the surrounding medium, with γ being the viscous coefficient of the medium. The second term represents the Lorentz force caused by the presence of a magnetic field [63] and the third term is the force exerted by the harmonic confinement. In addition, $\xi(t)$ is the noise term, which follows the Ornstein-Uhlenbeck process

$$t_c\dot{\xi}(t) = -\xi(t) + \eta(t), \quad (2)$$

with $\eta(t)$ being the delta-correlated white noise. Further, D is the strength of the Ornstein-Uhlenbeck noise [23,64,65]. Here $\xi(t)$ satisfies the properties

$$\langle\xi_\alpha(t)\rangle = 0, \quad \langle\xi_\alpha(t)\xi_\beta(t')\rangle = \frac{\delta_{\alpha\beta}}{2t_c}e^{-|t-t'|/t_c}, \quad (3)$$

where t_c is the noise correlation time or persistence time of the dynamics and $(\alpha, \beta) \in (X, Y)$. A finite correlation of noise for a time t_c represents the persistence of activity up to $t = t_c$ and it decays exponentially with t_c. Hence, a finite and nonzero t_c especially quantifies the activity of the system. In the limit $t_c \to 0$, the active fluctuation becomes thermal and the system becomes passive in nature. In the present work we consider $D = \gamma k_B T$ (fluctuation-dissipation relation) to have the typical thermal equilibrium limit of the dynamics at temperature T [66,67]. However, for a nonzero t_c, the dynamics is in nonequilibrium with an effective temperature which is different from the actual temperature of the system [68]. In the long time limit, one can define this effective temperature with the self-propulsion speed of the active particle and can relate it to the strength of noise, D [69].

By defining $\Gamma = \frac{\gamma}{m}$, $\omega_c = \frac{|q|B}{mc}$, and $\omega_0 = \sqrt{\frac{k}{m}}$ and introducing a complex variable $z(t) = x(t) + i\, y(t)$, Eq. (1) can be rewritten in terms of $z(t)$ as

$$\ddot{z}(t) + \Gamma\dot{z}(t) - j\omega_c\dot{z}(t) + \omega_0^2 z(t) = \epsilon(t), \quad (4)$$

where $j = \sqrt{-1}$ and $\epsilon(t) = \frac{\sqrt{2D}}{m}[\xi_x(t) + j\ \xi_y(t)]$. By performing the Laplace transform of the complex variables $z(t)$ and $\dot{z}(t)$ $[\mathcal{L}\{z\}(s) = \int_0^\infty e^{-st}z(t)dt$ and $\mathcal{L}\{\dot{z}\}(s) = \int_0^\infty e^{-st}\dot{z}(t)dt]$, with initial conditions $z(0) = z_0$ and $\dot{z}(0) = v_0$, respectively, and using the partial fraction method, the solution of the dynamics [Eq. (4)] can be obtained as

$$z(t) = \sum_{i=1}^{2} b_i z_0 e^{s_i t} + \sum_{i=1}^{2} a_i v_0 e^{s_i t} + \sum_{i=1}^{2} a_i \int_0^t e^{s_i(t-t')}\xi(t')dt'. \quad (5)$$

Here the s_i are given by

$$s_{1,2} = \frac{-\Omega \pm \sqrt{\Omega^2 - 4\omega_0^2}}{2},$$

with $\Omega = \Gamma - j\omega_c$. The coefficients a_i and b_i are given by

$$a_{1,2} = \pm\frac{1}{\sqrt{\Omega^2 - 4\omega_0^2}}, \quad b_{1,2} = \pm\frac{\Omega \mp \sqrt{\Omega^2 - 4\omega_0^2}}{2\sqrt{\Omega^2 - 4\omega_0^2}},$$

respectively. In order to analyze the transport behavior of such a system, we focus mainly on the mean displacement, steady-state correlations, and mean-square displacement. The mean displacement (MD) $\langle R(t)\rangle$ can be calculated from the relation

$$\begin{aligned}\langle R(t)\rangle &= \langle z(t) - z(0)\rangle \\ &= \langle x(t) - x(0)\rangle + j\langle y(t) - y(0)\rangle \\ &= a_1[e^{s_1 t}(s_1 z_0 + v_0 + \Omega z_0) \\ &\quad - e^{s_2 t}(s_2 z_0 + v_0 + \Omega z_0)] - z_0. \quad (6)\end{aligned}$$

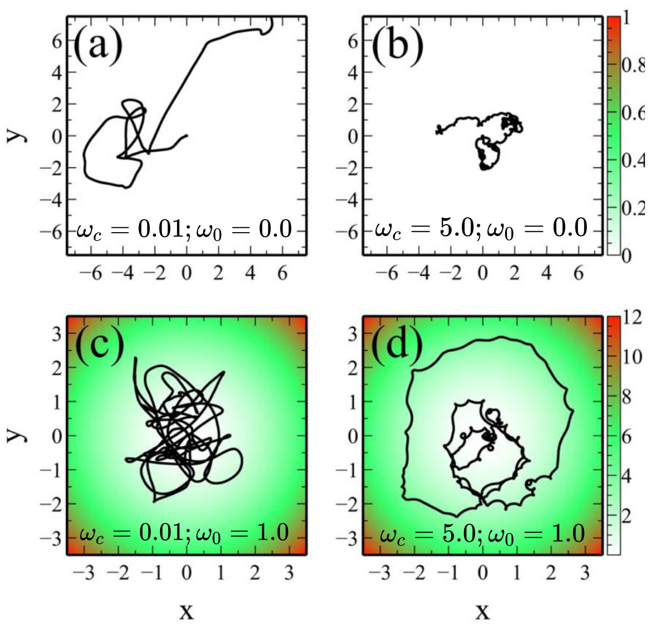

FIG. 1. Simulated trajectories of a free particle ($\omega_0 = 0$) in (a) and (b) and in the presence of harmonic confinement ($\omega_0 = 1.0$) in (c) and (d). The color map shows the strength of the harmonic confinement. Low magnetic field ($\omega_c = 0.01$) is considered for (a) and (c) while high magnetic field ($\omega_c = 5.0$) is taken for (b) and (d). The other common parameters are $m = 1$, $\gamma = 1.0$, and $t_c = 1.0$.

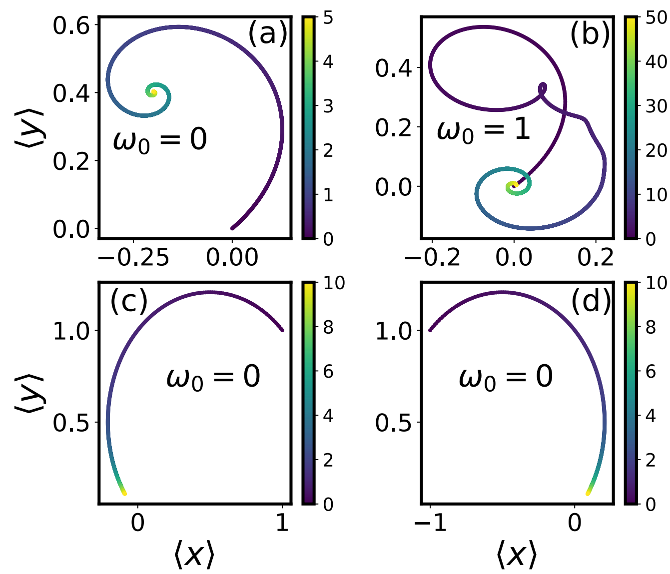

FIG. 2. The 2D parametric plot of MD [Eq. (10)] is shown in (a), (c), and (d) for a free particle ($\omega_0 = 0.0$) and in (b) for a confined harmonic particle ($\omega_0 = 1.0$). The color map indicates the evolution of MD with time in both (a) and (b). For a free particle, MD attains a non-zero stationary value in the long time limit or at the steady state. The color map in (c) and (d) represents the evolution of this stationary MD with ω_c and γ, respectively. The other common parameters in (c) are: $z_0 = 0 + 0j$, $t_c = 1.0$, $v_0 = 1 + j$, $m = 1$, and $\gamma = 1$. Similarly, the other common parameters in (d) are: $z_0 = 0 + 0j$, $t_c = 1.0$, $v_0 = 1 + j$, $m = 1$, and $\omega_c = 1$.

The steady-state position correlation [$C_r(t)$] and velocity correlation [$C_v(t)$] can be defined as

$$\begin{aligned} C_r(t) &= \lim_{t'\to\infty} \langle \mathbf{r}(t') \cdot \mathbf{r}(t'+t) \rangle \\ &= \lim_{t'\to\infty} \mathrm{Re}\{\langle z(t') z^*(t'+t) \rangle\} \end{aligned} \tag{7}$$

and

$$\begin{aligned} C_v(t) &= \lim_{t'\to\infty} \langle \mathbf{v}(t') \cdot \mathbf{v}(t'+t) \rangle \\ &= \lim_{t'\to\infty} \mathrm{Re}\{\langle \dot{z}(t') \dot{z}^*(t'+t) \rangle\}. \end{aligned} \tag{8}$$

In Eqs. (7) and (8) the asterisk denotes the complex conjugate and Re{ } represents the real part. Similarly, the mean-square displacement (MSD) $\langle R^2(t) \rangle$ is given by the relation

$$\begin{aligned} \langle R^2(t) \rangle &= \langle [\mathbf{r}(t) - \mathbf{r}_0]^2 \rangle \\ &= \langle |z(t) - z_0|^2 \rangle. \end{aligned} \tag{9}$$

The simulation of the dynamics [Eq. (1)] is carried out using Heun method algorithm [70] and Fox algorithm approaches [71]. A time step of 10^{-3} s is chosen for each run of the simulation. For each realization, the simulation is run up to 10^5 s. The averages are taken over 10^5 realizations after ignoring the initial transients (up to 10^3 s) in order for the system to reach the steady state. The detailed simulation results along with the analytical calculations are discussed in the following section.

III. RESULTS AND DISCUSSION

In Fig. 1 we show the simulated trajectories of the dynamics [Eq. (1)] for a free particle [Figs. 1(a) and 1(b)] and a harmonically confined particle [Figs. 1(c) and 1(d)]. The results presented in Figs. 1(a) and 1(c) are for a low-strength magnetic field ($\omega_c = 0.01$) whereas those in Figs. 1(b) and 1(d) are for a high-strength magnetic field ($\omega_c = 5.0$). It can be seen that in the absence of harmonic confinement ($\omega_0 = 0$), the particle is set as free and the influence of a strong magnetic field makes the particle confined to a very small region. In this case, the directional movement of the self-propelling particle is suppressed and the particle behaves as if it is trapped in the presence of a strong magnetic field [see Fig. 1(b)]. On the other hand, when the particle is confined in a harmonic trap, it cannot come out of the trap, and under the influence of the magnetic field, it moves around the field before returning to the mean position in the long time limit. When the strength of the magnetic field is very large, the particle moves around the field for a longer time and travels a larger distance [see Fig. 1(d)].

We have exactly calculated the mean displacement $\langle R(t) \rangle$ in the transient regime by expanding Eq. (6) in the lower powers of t as

$$\langle R(t) \rangle = v_0 t - \tfrac{1}{2}\left(v_0 \Omega - z_0 \omega_0^2\right) t^2 + O(t^3). \tag{10}$$

The parametric plot of MD [$\langle y(t) \rangle$ vs $\langle x(t) \rangle$] is shown in Fig. 2 when the particle is set free as well as when the particle is confined in a harmonic trap. The time asymptotic limit of the MD approaches zero value for a harmonically confined particle [$\lim_{t\to\infty} \langle R(t) \rangle = 0$] irrespective of the strength of the magnetic field. That is why in the long time limit the particle reaches the center of harmonic trap ($z = 0$), which is nothing but the initial position ($z = 0$) of the particle, as depicted in Fig. 2(b).

However, this is not the case for a free particle [Fig. 2(a)]. For a free particle, it is found that $\lim_{t\to\infty}\langle R(t)\rangle^{(f)} = \frac{v_0}{\Omega}$ and hence it depends on the magnetic field as well as on the viscosity of the medium. In the absence of a magnetic field, i.e., for the limit $\omega_c \to 0$, $\lim_{t\to\infty}\langle R(t)\rangle^{(f)} = \frac{v_0}{\Gamma}$, which reflects that the MD depends on the inertia of the particle. This is indeed consistent with the results reported in Ref. [72] for steady-state MD. Figures 2(c) and 2(d) depict the 2D plots of the variation of the steady-state MD with ω_c and γ, respectively. It starts from the value $\frac{v_0}{\Gamma}$ for $\omega_c = 0$ and approaches zero value for a strong magnetic field [Fig. 2(c)]. Similarly, it starts from the value $\frac{jv_0}{\omega_c}$ for $\gamma = 0$ and approaches zero for a larger value of γ [Fig. 2(d)]. This clearly indicates that the magnetic field has a strong influence on the MD only in the presence of inertia in the dynamics. In the absence of a magnetic field, the MD increases with inertia and approaches zero for the large-γ limit. It is also noteworthy that $\langle R(t)\rangle$ does not depend on the activity time or persistence time of the dynamics. This is because of the definition of statistical properties of the AOUP noise. In the lower time regime (the limit $t \to 0$), the MD varies linearly with time and depends only on the initial velocity of the particle.

Next we examine the steady-state behavior of the position correlation $C_r(t)$ and velocity correlation $C_v(t)$. Substituting the solution $z(t)$ from Eq. (5) and the noise properties from Eq. (3) in Eq. (7), $C_r(t)$ can be calculated as

$$C_r(t) = \mathrm{Re}\left\{\sum_{i=1}^{2}\sum_{j=1}^{2}\frac{2a_i a_j^* D}{m^2}\left(\frac{t_c e^{-t/tc}}{(t_c s_i - 1)(t_c s_j^* + 1)} - \frac{2e^{s_j^* t}}{(s_i + s_j^*)(1 - t_c^2 s_j^{*2})}\right)\right\}. \tag{11}$$

Similarly, substituting the solution $z(t)$ from Eq. (5) and the noise properties from Eq. (3) in Eq. (8), $C_v(t)$ can be calculated as

$$C_v(t) = \mathrm{Re}\left\{\sum_{i=1}^{2}\sum_{j=1}^{2}\frac{2c_i c_j^* D}{m^2}\left(\frac{t_c e^{-t/tc}}{(t_c s_i - 1)(t_c s_j^* + 1)} - \frac{2e^{s_j^* t}}{(s_i + s_j^*)(1 - t_c^2 s_j^{*2})}\right)\right\}, \tag{12}$$

where

$$c_{1,2} = \frac{-\Omega \pm \sqrt{\Omega^2 - 4\omega_0^2}}{\sqrt{\Omega^2 - 4\omega_0^2}}. \tag{13}$$

For a confined harmonic particle, the normalized $C_r(t)$ and $C_v(t)$ are plotted as a function of t in Fig. 3 for different values of ω_c. The results presented in Figs. 3(a) and 3(b) for $C_r(t)$ are for inertial ($\gamma = 1$) and overdamped ($\gamma = 10$) regimes, respectively. Similarly, the results presented in Figs. 3(c) and 3(d) for $C_v(t)$ are for inertial ($\gamma = 1$) and overdamped ($\gamma = 10$) regimes, respectively. The obtained analytical results are in good agreement with the simulation. It is observed that with an increase in magnetic field strength ω_c, the correlation in position persists for a longer time before decaying to zero, whereas the velocity correlation decays faster with ω_c, as

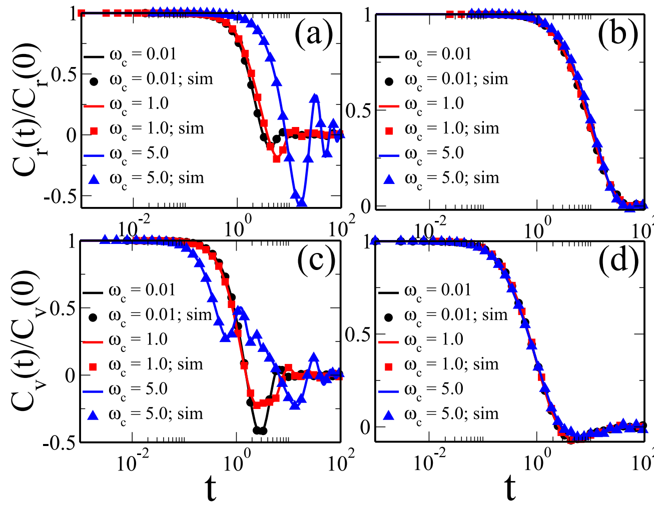

FIG. 3. Normalized $C_r(t)$ [Eq. (11)] as a function of t is shown in (a) and (b) and normalized $C_v(t)$ [Eq. (12)] as a function of t is shown in (c) and (d), respectively for a confined harmonic particle ($\omega_0 = 1$), obtained from the analytical calculations as well as from the simulation for different values of ω_c. We have taken $\gamma = 1.0$ in (a) and (c) and $\gamma = 10.0$ in (b) and (d). The other common parameters are $t_c = 1$ and $m = 1$.

expected. Most importantly, in the overdamped regime ($\gamma = 10$), where the inertial effects are negligible, the magnetic field does not influence the correlated behavior of either position or velocity.

The dependence of steady-state correlations on harmonic confinement ω_0 and correlation time t_c are shown in Fig. 4. Both $C_r(t)$ and $C_v(t)$ decay faster with an increase in ω_0,

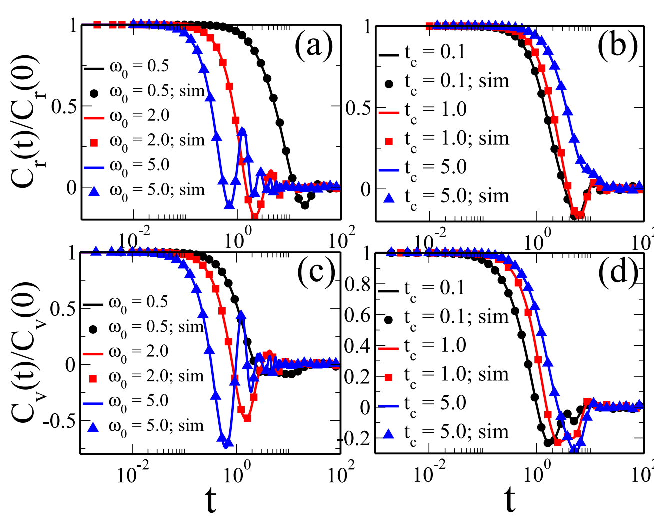

FIG. 4. Normalized $C_r(t)$ [Eq. (11)] as a function of t obtained from both analytical calculations and simulation for different values of ω_0 and t_c are shown in (a) and (b), respectively. Normalized $C_v(t)$ [Eq. (12)] as a function of t obtained from both analytical calculations and simulation for different values of ω_0 and t_c are shown in (c) and (d), respectively. We have taken $t_c = 1$ in (a) and (c) and $\omega_0 = 1.0$ in (b) and (d). The other common parameters are $\omega_c = 1$, $m = 1$, and $\gamma = 1$.

whereas with an increase in t_c, both quantities persist for a longer time before decaying to zero.

Using Eq. (5) in Eq. (9), the MSD of the harmonically confined particle $\langle R^2(t)\rangle$ can exactly be calculated as

$$\langle R^2(t)\rangle = \left|a_1\left(-\frac{z_0}{a_1}+(e^{s_1t}-e^{s_2t})(v_0+\Omega z_0)+s_1z_0e^{s_1t}-s_2z_0e^{s_2t}\right)\right|^2+\sum_i\sum_j\frac{2a_ia_j^*D}{m^2} \times\left(\frac{t_ce^{t(s_j^*-1/t_c)}}{(t_cs_i+1)(1-t_cs_j^*)}+\frac{t_ce^{t(s_i-1/t_c)}}{(1-t_cs_i)(t_cs_j^*+1)}+\frac{t_c(s_i+s_j^*)-2}{(s_i+s_j^*)(t_cs_i-1)(t_cs_j^*-1)}+\frac{e^{t(s_i+s_j^*)}(t_c(s_i+s_j^*)+2)}{(s_i+s_j^*)(t_cs_i+1)(t_cs_j^*+1)}\right). \tag{14}$$

With the help of Taylor series expansion, Eq. (14) can be expanded in the powers of t and by dropping the higher powers of t, $\langle R^2(t)\rangle$ can be obtained as

$$\langle R^2(t)\rangle = |v_0|^2t^2-\frac{|v_0|^2+2(v_0^*z_0+v_0z_0^*)\omega_0^2}{2}t^3 +\frac{1}{12}\left(\frac{6D}{m^2t_c}+\omega_0^2(5\Gamma-j\omega_c)(v_0z_0^*+z_0v_0^*)+3|z_0|^2\omega_0^4+|v_0|^2\left(7\Gamma^2-4\omega_0^2-\omega_c^2\right)\right)t^4+O(t^5). \tag{15}$$

We have plotted the MSD as a function of t for a free particle and for a confined harmonic particle in Figs. 5(a) and 5(b), respectively, for different values of ω_c. From the exact calculation of the MSD, it is confirmed that in the limit $t\to 0$, $\langle R^2(t)\rangle$ is proportional to t^2, and hence the dynamics is ballistic in nature. The initial ballistic regime (proportional to t^2) depends solely on the initial velocity v_0 of the particle. When $v_0=0$, the initial regime of the MSD is proportional to t^4. The dependence of the MSD on ω_c appears, starting from the fourth power of t. Since there is harmonic confinement, the particle cannot escape to infinity. Hence, in the long time regime, the MSD attains a constant or saturated value $\langle R^2\rangle_{st}$ [see Fig. 5(b)], which is given by the expression

$$\langle R^2\rangle_{\rm st} = |z_0|^2+\frac{2D\left[t_c^2\left(\omega_c^2+\Gamma^2+\omega_0^2\right)\right]}{\Gamma m^2\omega_0^2\left\{\left[t_c\left(\omega_0^2t_c+\Gamma\right)+1\right]^2+t_c^2\omega_c^2\right\}}+\frac{2D\left(\Gamma\omega_0^2t_c^3+2\Gamma t_c+1\right)}{\Gamma m^2\omega_0^2\left\{\left[t_c\left(\omega_0^2t_c+\Gamma\right)+1\right]^2+t_c^2\omega_c^2\right\}}. \tag{16}$$

This saturated value of the MSD depends on ω_c. In the limit $\omega_c\to 0$, $\langle R^2\rangle_{\rm st}$ is obtained as

$$\lim_{\omega_c\to 0}\langle R^2\rangle_{\rm st} = |z_0|^2+\frac{2D(1+t_c\Gamma)}{m^2\omega_0^2[\Gamma+t_c\Gamma\left(\Gamma+t_c\omega_0^2\right)]}, \tag{17}$$

which is the same as that reported in Ref. [72] in the absence of a magnetic field. In the presence of a very strong magnetic field, i.e., in the limit $\omega_c\to\infty$, the stationary MSD is simply $|z_0|^2+\frac{2D}{m^2\Gamma\omega_0^2}$, which is independent of t_c. The same value of $\langle R^2\rangle_{\rm st}$ is obtained when we take the white noise limit, i.e., in the limit $t_c\to 0$. This confirms that the particle behaves like a passive particle in the presence of a high magnetic field. In the thermal equilibrium limit of our model, the MSD shows behavior similar to that reported in Ref. [58]. It is also observed that $\langle R^2\rangle_{\rm st}$ is an increasing function of ω_c, and hence the magnetic field enhances the overall displacement for a confined harmonic particle. This is clearly reflected in Fig. 5(b).

The MSD for a free particle $\langle R^2(t)\rangle^{(f)}$ can be calculated by substituting $\omega_0=0$ and simplifying Eq. (14) as

$$\langle R^2(t)\rangle^{(f)} = \frac{2|v_0|^2e^{-\Gamma t}[\cosh(\Gamma t)-\cos(\omega_ct)]}{\Gamma^2+\omega_c^2}+\frac{2D}{m^2(\Gamma^2+\omega_c^2)} \times\left(\frac{e^{-\Gamma t}\left\{2\cos(\omega_ct)\left[t_c\omega_c^2(\Gamma t_c+1)+\Gamma(\Gamma t_c-2)(\Gamma t_c-1)\right]-2\omega_c\sin(\omega_ct)\left[t_c^2\left(\Gamma^2+\omega_c^2\right)-4\Gamma t_c+2\right]\right\}}{\left(\Gamma^2+\omega_c^2\right)\left[t_c^2\omega_c^2+(\Gamma t_c-1)^2\right]}\right. + \frac{2t_c^2e^{-t(\Gamma+1/t_c)}\left\{\omega_c\sin(\omega_ct)\left[t_c^2\left(\Gamma^2+\omega_c^2\right)-2\Gamma t_c-1\right]+\cos(\omega_ct)\left[-\Gamma\left(\Gamma^2t_c^2-1\right)-t_c\omega_c^2(\Gamma t_c+2)\right]\right\}}{\left[t_c^2\omega_c^2+(\Gamma t_c-1)^2\right]\left[t_c^2\omega_c^2+(\Gamma t_c+1)^2\right]} \left.-\frac{4\Gamma}{\Gamma^2+\omega_c^2}+\frac{2t_ce^{-t/t_c}(\Gamma t_c-1)}{t_c^2\omega_c^2+(\Gamma t_c-1)^2}+\frac{e^{-2\Gamma t}(\Gamma t_c-1)}{\Gamma\left[t_c^2\omega_c^2+(\Gamma t_c-1)^2\right]}+\frac{(\Gamma t_c+1)(2\Gamma t_c+1)}{\Gamma\left[t_c^2\omega_c^2+(\Gamma t_c+1)^2\right]}+2t-2t_c+2t_ce^{-t/t_c}\right). \tag{18}$$

Expanding Eq. (18) in powers of t, we get

$$\langle R^2(t)\rangle^{(f)} = |v_0|^2t^2-\Gamma|v_0|^2t^3+\left(\frac{D}{2m^2t_c}+\frac{7\Gamma^2|v_0|^2}{12}-\frac{|v_0|^2\omega_c^2}{12}\right)t^4+O(t^5). \tag{19}$$

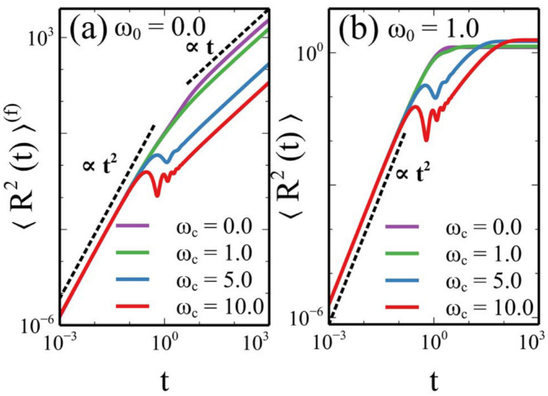

FIG. 5. MSD as a function of t for different ω_c values (a) for a free particle [Eq. (18)] and (b) for a confined harmonic particle [Eq. (14)]. The other common parameters are $t_c = 1$, $\gamma = 1$, and $m = 1$.

From this equation it is confirmed that $\langle R^2(t)\rangle^{(f)}$ depends on the magnetic field and in the absence of a magnetic field (the limit $\omega_c \to 0$), the result for $\langle R^2(t)\rangle^{(f)}$ is consistent with that reported for a free particle in Ref. [72]. In the time asymptotic limit ($t \to \infty$), the MSD in Eq. (18) reduces to

$$\langle R^2\rangle_{\rm st}^{(f)} = \frac{2D}{m^2(\Gamma^2+\omega_c^2)}\Bigg(-\frac{4\Gamma}{\Gamma^2+\omega_c^2} + 2t - 2t_c + \frac{(\Gamma t_c+1)(2\Gamma t_c+1)}{\Gamma\big[t_c^2\omega_c^2 + (\Gamma t_c+1)^2\big]}\Bigg). \tag{20}$$

Thus, the steady-state MSD for a free particle depends on ω_c and approaches zero in the limit $\omega_c \to \infty$. This indicates that the presence of a magnetic field suppresses the overall displacement of a free particle in contrast to that of a harmonically confined particle. These results are summarized in Fig. 5, where it can be seen that the initial ballistic regimes are similar for both the free and the confined harmonic particle. However, in the long time regime, the MSD is linearly proportional to t for a free particle (diffusive in nature) but it approaches a stationary value for a confined harmonic particle (nondiffusive in nature). The steady-state MSD for a free particle gets suppressed with the magnetic field, whereas it gets enhanced for a confined harmonic particle. Other than these, we observe oscillations in the intermediate time regimes for both free and harmonically confined particles, which could be due to the influence of the magnetic field. It should also be noted that in the limit $t_c \to \infty$ (with $t \gg t_c$), $\langle R^2\rangle_{\rm st}^{(f)}$ can be obtained as

$$\lim_{t_c\to\infty}\langle R^2\rangle_{\rm st}^{(f)} = \frac{2D}{m^2(\Gamma^2+\omega_c^2)}\left(-\frac{2\Gamma}{\Gamma^2+\omega_c^2} + 2t\right), \tag{21}$$

which is independent of t_c.

The MSD as a function of t is plotted for different Γ and t_c values in Figs. 6(a) and 6(b) for a confined harmonic particle and in Figs. 6(c) and 6(d) for a free particle, respectively. It can be seen that for a free particle in the time asymptotic limit, the MSD is independent of t_c, while for a confined harmonic particle, t_c suppresses the MSD. However, for both free and harmonically confined particles, the MSD gets suppressed with Γ. Since the MSD for a free particle in the time asymptotic limit is proportional to t, the steady-state diffusion coefficient for a free particle $\mathcal{D}_f$ can be calculated as

$$\mathcal{D}_f = \lim_{t\to\infty}\frac{\langle R^2(t)\rangle^{(f)}}{2t} = \frac{2D}{\gamma^2+m^2\omega_c^2}. \tag{22}$$

Substituting $\omega_c = \frac{qB}{mc}$ in the above equation, $\mathcal{D}_f$ can be simplified as

$$\mathcal{D}_f = \frac{2Dc^2}{\gamma^2c^2+q^2B^2}. \tag{23}$$

Hence, $\mathcal{D}_f$ is independent of the mass of the particle but it depends on the magnetic field. It approaches zero when the particle is subjected to a strong magnetic field. In the equilibrium limit ($D = \gamma k_B T$), the diffusive behavior is found to be similar to that reported in Ref. [57], and in the absence of a magnetic field, the expression of D_f is the same as that reported in Ref. [72].

IV. SUMMARY

In this work we have studied the motion of a charged inertial active Ornstein-Uhlenbeck particle in the presence of

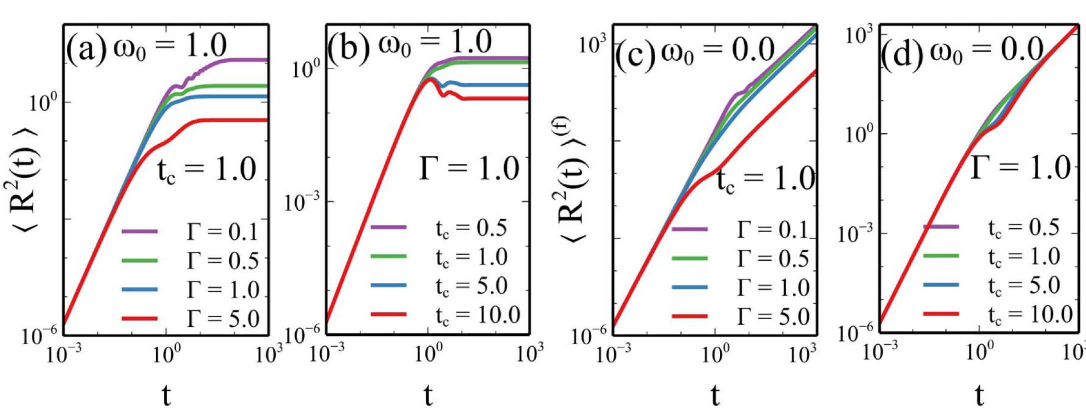

FIG. 6. For a harmonically confined particle ($\omega_0 = 1.0$), MSD as a function of t [Eq. (14)] (a) for different Γ values fixing $t_c = 1.0$ and (b) for different t_c values fixing $\Gamma = 1.0$. For a free particle, MSD as a function of t [Eq. (18)] (c) for different Γ values fixing $t_c = 1$ and (d) for different t_c values fixing $\Gamma = 1.0$. The common parameters are $\omega_c = 1.0$ and $m = 1.0$.

a magnetic field. One of the important observations is that the magnetic field has a strong influence on the dynamical behavior of the particle because of the presence of inertia in the dynamics. The particle (if free) on average covers a finite distance before settling down at a constant value in the long time limit. This constant value is found to be dependent on the magnetic field, which decreases with an increase in field strength. In contrast, if the particle is confined in a harmonic trap, it always returns to the mean position of the trap, irrespective of the magnetic field. For a highly viscous medium, where the inertial influence is negligible, the dynamical behavior of the particle is not affected by the magnetic field. Furthermore, the initial time regime of the mean-square displacement is found to be similar and shows ballistic behavior for both free and confined harmonic particles. On the other hand, the time asymptotic regime is diffusive for a free particle and nondiffusive for a harmonic particle. The ballistic regime for both free and confined harmonic particles gets reduced with an increase in the magnetic field strength.

Surprisingly, for a harmonically confined particle, the steady-state mean-square displacement in the presence of a very strong magnetic field is the same as that for a passive particle. When the strength of the magnetic field is very high, the steady-state mean-square displacement becomes independent of the field as well as the noise correlation time or persistent time of the dynamics, ensuring that the particle behaves like a passive particle. To understand this feature, it is further necessary to explore the relaxation behavior of the dynamics and quantify the degree of irreversibility in terms of entropy production and nonequilibrium temperature [66,67]. Similarly, for a free particle, in the time asymptotic limit, the MSD becomes independent of activity despite the persistence of activity for a longer time.

We believe that the results of our model are amenable to experimental verification and can be applied to implement the magnetic control on a charged active suspension by fine-tuning the strength of the external magnetic field. It would be further interesting to explore the relaxation behavior of the dynamics by introducing elasticity in the viscous solution [64,73]. Moreover, the inertial AOUP under the action of a magnetic field can be extended to a more complex situation as in Refs. [54,55].

ACKNOWLEDGMENTS

M.S. acknowledges start up grant from the Faculty Recharge Program (FRP-56055) of UGC, Government of India for financial support.

[1] C. Bechinger, R. Di Leonardo, H. Löwen, C. Reichhardt, G. Volpe, and G. Volpe, Active particles in complex and crowded environments, Rev. Mod. Phys. **88**, 045006 (2016).

[2] S. Ramaswamy, Active matter, J. Stat. Mech. (2017) 054002.

[3] P. Pietzonka, The oddity of active matter, Nat. Phys. **17**, 1193 (2021).

[4] G. De Magistris and D. Marenduzzo, An introduction to the physics of active matter, Physica A **418**, 65 (2015).

[5] C. Dombrowski, L. Cisneros, S. Chatkaew, R. E. Goldstein, and J. O. Kessler, Self-Concentration and Large-Scale Coherence in Bacterial Dynamics, Phys. Rev. Lett. **93**, 098103 (2004).

[6] H. C. Berg and D. A. Brown, Chemotaxis in *Escherichia coli* analysed by three-dimensional tracking, Nature (London) **239**, 500 (1972).

[7] H. Machemer, Ciliary activity and the origin of metachrony in paramecium: Effects of increased viscosity, J. Exp. Biol. **57**, 239 (1972).

[8] C. Jones, M. Gomez, R. M. Muoio, A. Vidal, R. A. Mcknight, N. D. Brubaker, and W. W. Ahmed, Stochastic force dynamics of the model microswimmer *Chlamydomonas reinhardtii*: Active forces and energetics, Phys. Rev. E **103**, 032403 (2021).

[9] A. Walther and A. H. E. Müller, Janus particles: Synthesis, self-assembly, physical properties, and applications, Chem. Rev. **113**, 5194 (2013).

[10] J. R. Howse, R. A. L. Jones, A. J. Ryan, T. Gough, R. Vafabakhsh, and R. Golestanian, Self-Motile Colloidal Particles: From Directed Propulsion to Random Walk, Phys. Rev. Lett. **99**, 048102 (2007).

[11] C. Scholz, M. Engel, and T. Pöschel, Rotating robots move collectively and self organize, Nat. Commun. **9**, 931 (2018).

[12] B. ten Hagen, S. van Teeffelen, and H. Lowen, Non-Gaussian behaviour of a self-propelled particle on a substrate, Condens. Matter Phys. **12**, 725 (2009).

[13] B. ten Hagen, S. van Teeffelen, and H. Löwen, Brownian motion of a self-propelled particle, J. Phys.: Condens. Matter **23**, 194119 (2011).

[14] M. E. Cates and J. Tailleur, When are active Brownian particles and run-and-tumble particles equivalent? Consequences for motility-induced phase separation, Europhys. Lett. **101**, 20010 (2013).

[15] K. Malakar, A. Das, A. Kundu, K. V. Kumar, and A. Dhar, Steady state of an active Brownian particle in a two-dimensional harmonic trap, Phys. Rev. E **101**, 022610 (2020).

[16] H. Löwen, Inertial effects of self-propelled particles: From active Brownian to active Langevin motion, J. Chem. Phys. **152**, 040901 (2020).

[17] B. Lehle and J. Peinke, Analyzing a stochastic process driven by Ornstein-Uhlenbeck noise, Phys. Rev. E **97**, 012113 (2018).

[18] L. L. Bonilla, Active Ornstein-Uhlenbeck particles, Phys. Rev. E **100**, 022601 (2019).

[19] D. Martin, J. O'Byrne, M. E. Cates, É. Fodor, C. Nardini, J. Tailleur, and F. van Wijland, Statistical mechanics of active Ornstein-Uhlenbeck particles, Phys. Rev. E **103**, 032607 (2021).

[20] G. Szamel, Self-propelled particle in an external potential: Existence of an effective temperature, Phys. Rev. E **90**, 012111 (2014).

[21] C. Sandford, A. Y. Grosberg, and J.-F. Joanny, Pressure and flow of exponentially self-correlated active particles, Phys. Rev. E **96**, 052605 (2017).

[22] U. M. B. Marconi, C. Maggi, and M. Paoluzzi, Pressure in an exactly solvable model of active fluid, J. Chem. Phys. **147**, 024903 (2017).

[23] S. Das, G. Gompper, and R. G. Winkler, Confined active Brownian particles: Theoretical description of propulsion-induced accumulation, New J. Phys. **20**, 015001 (2018).

[24] R. Wittmann, J. M. Brader, A. Sharma, and U. M. B. Marconi, Effective equilibrium states in mixtures of active particles driven by colored noise, Phys. Rev. E **97**, 012601 (2018).
[25] L. Caprini, U. M. B. Marconi, and A. Vulpiani, Linear response and correlation of a self-propelled particle in the presence of external fields, J. Stat. Mech. (2018) 033203.
[26] L. Caprini and U. M. B. Marconi, Time-dependent properties of interacting active matter: Dynamical behavior of one-dimensional systems of self-propelled particles, Phys. Rev. Research **2**, 033518 (2020).
[27] U. M. B. Marconi and C. Maggi, Towards a statistical mechanical theory of active fluids, Soft Matter **11**, 8768 (2015).
[28] G. Gompper, R. G. Winkler, T. Speck, A. Solon, C. Nardini, F. Peruani, H. Löwen, R. Golestanian, U. B. Kaupp, L. Alvarez, T. Kiørboe, E. Lauga, W. C. K. Poon, A. DeSimone, S. Muiños-Landin, A. Fischer, N. A. Söker, F. Cichos, R. Kapral, P. Gaspard *et al.*, The 2020 motile active matter roadmap, J. Phys.: Condens. Matter **32**, 193001 (2020).
[29] M. E. Cates and J. Tailleur, Motility-induced phase separation, Annu. Rev. Condens. Matter Phys. **6**, 219 (2015).
[30] M. Gazzola, M. Argentina, and L. Mahadevan, Scaling macroscopic aquatic locomotion, Nat. Phys. **10**, 758 (2014).
[31] M. Saadat, F. E. Fish, A. G. Domel, V. Di Santo, G. V. Lauder, and H. Haj-Hariri, On the rules for aquatic locomotion, Phys. Rev. Fluids **2**, 083102 (2017).
[32] M. Gazzola, M. Argentina, and L. Mahadevan, Gait and speed selection in slender inertial swimmers, Proc. Natl. Acad. Sci. USA **112**, 3874 (2015).
[33] S. P. Sane, The aerodynamics of insect flight, J. Exp. Biol. **206**, 4191 (2003).
[34] L. Caprini and U. M. B. Marconi, Inertial self-propelled particles, J. Chem. Phys. **154**, 024902 (2021).
[35] L. Caprini and U. M. B. Marconi, Spatial velocity correlations in inertial systems of active Brownian particles, Soft Matter **17**, 4109 (2021).
[36] C. Scholz, S. Jahanshahi, A. Ldov, and H. Löwen, Inertial delay of self propelled particles, Nat. Commun. **9**, 5156 (2018).
[37] O. Dauchot and V. Démery, Dynamics of a Self-Propelled Particle in a Harmonic Trap, Phys. Rev. Lett. **122**, 068002 (2019).
[38] S. Mandal, B. Liebchen, and H. Löwen, Motility-Induced Temperature Difference in Coexisting Phases, Phys. Rev. Lett. **123**, 228001 (2019).
[39] J. Singh and S. Dattagupta, Stochastic motion of a charged particle in a magnetic field: I classical treatment, Pramana **47**, 199 (1996).
[40] A. Jayannavar and N. Kumar, Orbital diamagnetism of a charged Brownian particle undergoing a birth-death process, J. Phys. A: Math. Gen. **14**, 1399 (1981).
[41] A. Saha and A. M. Jayannavar, Nonequilibrium work distributions for a trapped Brownian particle in a time-dependent magnetic field, Phys. Rev. E **77**, 022105 (2008).
[42] J. I. Jiménez-Aquino, R. M. Velasco, and F. J. Uribe, Fluctuation relations for a classical harmonic oscillator in an electromagnetic field, Phys. Rev. E **79**, 061109 (2009).
[43] T. Harko and G. Mocanu, Electromagnetic radiation of charged particles in stochastic motion, Eur. Phys. J. C **76**, 160 (2016).
[44] F.-j. Lin, J.-j. Liao, and B.-q. Ai, Separation and alignment of chiral active particles in a rotational magnetic field, J. Chem. Phys. **152**, 224903 (2020).
[45] D. Jin and L. Zhang, Collective behaviors of magnetic active matter: Recent progress toward reconfigurable, adaptive, and multifunctional swarming micro/nanorobots, Acc. Chem. Res. **55**, 98 (2022).
[46] *Niels Bohr: Collected Works: Early Work (1905–1911)*, edited by L. Rosenfeld and J. R. Nielsen (North-Holland, Amsterdam, 1972).
[47] H.-J. Van Leeuwen, Problemes de la théorie électronique du magnétisme, J. Phys. Radium **2**, 361 (1921).
[48] S. Dattagupta and J. Singh, Landau Diamagnetism in a Dissipative and Confined System, Phys. Rev. Lett. **79**, 961 (1997).
[49] A. M. Jayannavar and M. Sahoo, Charged particle in a magnetic field: Jarzynski equality, Phys. Rev. E **75**, 032102 (2007).
[50] R. Kubo, The fluctuation-dissipation theorem, Rep. Prog. Phys. **29**, 255 (1966).
[51] N. Kumar, Classical orbital magnetic moment in a dissipative stochastic system, Phys. Rev. E **85**, 011114 (2012).
[52] M. Muhsin, M. Sahoo, and A. Saha, Orbital magnetism of an active particle in viscoelastic suspension, Phys. Rev. E **104**, 034613 (2021).
[53] M. Sandoval, R. Velasco, and J. Jiménez-Aquino, Magnetic field effect on charged Brownian swimmers, Physica A **442**, 321 (2016).
[54] H. D. Vuijk, J. U. Sommer, H. Merlitz, J. M. Brader, and A. Sharma, Lorentz forces induce inhomogeneity and flux in active systems, Phys. Rev. Research **2**, 013320 (2020).
[55] I. Abdoli and A. Sharma, Stochastic resetting of active Brownian particles with Lorentz force, Soft Matter **17**, 1307 (2021).
[56] Karmeshu, Brownian motion of charged particles in a magnetic field, Phys. Fluids **17**, 1828 (1974).
[57] F. N. C. Paraan, M. P. Solon, and J. P. Esguerra, Brownian motion of a charged particle driven internally by correlated noise, Phys. Rev. E **77**, 022101 (2008).
[58] V. Lisy and J. Tothova, Brownian motion of charged particles driven by correlated noise in magnetic field, Transp. Theory Stat. Phys. **42**, 365 (2013).
[59] A. Baura, S. Ray, M. Kumar Sen, and B. Chandra Bag, Study of non-Markovian dynamics of a charged particle in presence of a magnetic field in a simple way, J. Appl. Phys. **113**, 124905 (2013).
[60] V. Lisý and J. Tóthová, Effect of magnetic field on the fluctuations of charged oscillators in viscoelastic fluids, Acta Phys. Pol. A **126**, 413 (2014).
[61] J. Das, S. Mondal, and B. C. Bag, Fokker-Planck equation for the non-Markovian Brownian motion in the presence of a magnetic field, J. Chem. Phys. **147**, 164102 (2017).
[62] A. Noushad, S. Shajahan, and M. Sahoo, Velocity auto correlation function of a confined Brownian particle, Eur. Phys. J. B **94**, 202 (2021).
[63] J. C. Maxwell, *A Treatise on Electricity and Magnetism* (Clarendon, Oxford, 1873), Vol. 1.
[64] F. J. Sevilla, R. F. Rodríguez, and J. R. Gomez-Solano, Generalized Ornstein-Uhlenbeck model for active motion, Phys. Rev. E **100**, 032123 (2019).
[65] E. Woillez, Y. Kafri, and V. Lecomte, Nonlocal stationary probability distributions and escape rates for an active Ornstein-Uhlenbeck particle, J. Stat. Mech. (2020) 063204.

[66] É. Fodor, C. Nardini, M. E. Cates, J. Tailleur, P. Visco, and F. van Wijland, How Far from Equilibrium Is Active Matter?, Phys. Rev. Lett. **117**, 038103 (2016).

[67] D. Mandal, K. Klymko, and M. R. DeWeese, Entropy Production and Fluctuation Theorems for Active Matter, Phys. Rev. Lett. **119**, 258001 (2017).

[68] J. Tailleur and M. E. Cates, Sedimentation, trapping, and rectification of dilute bacteria, Europhys. Lett. **86**, 60002 (2009).

[69] Y. Fily and M. C. Marchetti, Athermal Phase Separation of Self-Propelled Particles with No Alignment, Phys. Rev. Lett. **108**, 235702 (2012).

[70] T. G. G. Gard, *Introduction to Stochastic Differential Equations* (Dekker, New York, 1988).

[71] R. F. Fox, I. R. Gatland, R. Roy, and G. Vemuri, Fast, accurate algorithm for numerical simulation of exponentially correlated colored noise, Phys. Rev. A **38**, 5938 (1988).

[72] G. H. P. Nguyen, R. Wittmann, and H. Löwen, Active Ornstein-Uhlenbeck model for self-propelled particles with inertia, J. Phys.: Condens. Matter **34**, 035101 (2022).

[73] I. Goychuk, in *Advances in Chemical Physics*, edited by S. A. Rice and A. R. Dinner (Wiley, New York, 2012), pp. 187–253.